0273-2289/1559-0291 (Online)/06/128/0237/$30.00

Transcription Analysis of Recombinant *Saccharomyces cerevisiae* Reveals Novel Responses to Xylose

Laura Salusjärvi,* Juha-Pekka Pitkänen, Aristos Aristidou, Laura Ruohonen, and Merja Penttilä

VTT Biotechnology, PO Box 1500, FIN-02044 VTT, Finland,
E-mail: laura.salusjarvi@vtt.fi

Received July 7, 2005; Revised September 5, 2005;
Accepted September 9, 2005

Abstract

Lignocellulosic biomass, rich in hexose and pentose sugars, is an attractive resource for commercially viable bioethanol production. *Saccharomyces cerevisiae* efficiently ferments hexoses but is naturally unable to utilize pentoses. Metabolic engineering of this yeast has resulted in strains capable of xylose utilization. However, even the best recombinant *S. cerevisiae* strains of today metabolize xylose with a low rate compared to glucose. This study compares the transcript profiles of an *S. cerevisiae* strain engineered to utilize xylose via the xylose reductase–xylitol dehydrogenase pathway in aerobic chemostat cultures with glucose or xylose as the main carbon source. Compared to the glucose culture, 125 genes were upregulated, whereas 100 genes were downregulated in the xylose culture. A number of genes encoding enzymes capable of nicotinamide adenine dinucleotide phosphate regeneration were upregulated in the xylose culture. Furthermore, xylose provoked increased activities of the pathways of acetyl-CoA synthesis and sterol biosynthesis. Notably, our results suggest that cells metabolizing xylose are not in a completely repressed or in a derepressed state either, indicating that xylose was recognized neither as a fermentable nor as a respirative carbon source. In addition, a considerable number of the changes observed in the gene expression between glucose and xylose samples were closely related to the starvation response.

Index Entries: Xylose; transcriptional profiling; ethanol; metabolic engineering; *Saccharomyces cerevisiae*.

*Author to whom all correspondence and reprint requests should be addressed.

Introduction

Saccharomyces cerevisiae is one of the most efficient hexose-fermenting organisms, and this capability has been exploited for hundreds of years for ethanol production. By contrast, the interest in xylose utilization by this yeast has arisen more recently, along with the call for an efficient industrial conversion of lignocellulosic materials into fuels and other products. *S. cerevisiae* cannot naturally ferment xylose, but its metabolic engineering for xylose fermentation has progressively advanced. The most common strategy has been the expression of genes for xylose reductase (XR) (*XYL1*) and xylitol dehydrogenase (XDH) (*XYL2*) of *Pichia stipitis (1)* and the overexpression of the gene encoding the endogenous xylulokinase (XK) (*XKS1*) *(2–5)*. As a result of these efforts, fermentation of xylose is enabled in *S. cerevisiae*, but the ethanol production rate and yield over the carbon utilized are still significantly lower than with hexose sugars. Various approaches in different laboratories have been taken to address this inefficiency. These include fine tuning of the expression levels of *XYL1*, *XYL2*, and *XKS1 (6,7)*; construction of XR–XDH fusion proteins *(8)*; mutagenesis of recombinant xylose-fermenting strains *(9,10)*; overexpression of genes encoding enzymes of the nonoxidative pentose phosphate pathway (PPP) *(11)*; and deletion of genes encoding enzymes of the oxidative PPP *(12,13)* to increase or decrease, respectively, the carbon flux through these metabolic branches of the PPP. Moreover, xylose consumption was improved in a recombinant *S. cerevisiae* strain by alleviation of carbon catabolite repression *(14)*.

The two-step oxidoreductase reaction catalyzed by XR and XDH enzymes is overall redox neutral but requires different cofactors, because XR prefers nicotinamide adenine dinucleotide phosphate (NADPH) to NADH and XDH solely utilizes NAD^+. This is postulated to lead to an imbalance in the cofactor pools, which disturbs the redox state of the cells during the metabolism of xylose. Thus, attempts to modify the cofactor specificity of XR and XDH have been reported *(15–18)*. Other strategies to balance the cellular redox include efforts to increase the availability of intracellular NADPH by metabolic engineering of ammonium assimilation pathways *(19)*, or by overexpression of a fungal $NADP^+$-dependent D-glyceraldehyde-3-phosphate dehydrogenase *(13)*. Furthermore, transhydrogenase-like futile cycles using endogenous enzyme activities of yeast have been constructed in the xylose-metabolizing *S. cerevisiae* to alleviate the redox imbalance *(20)*. Recently, approaches to circumvent the redox issue of xylose conversion by the oxidoreductive pathway met with significant success by Kuyper et al. *(21,22)*, who expressed a fungal xylose isomerase in *S. cerevisiae*. Anaerobic ethanol yield on xylose, 0.42 g/g, was approx 80% of the theoretical maximum with this strain. However, the rate of xylose consumption still remained significantly lower compared to glucose, as did the growth rate both aerobically and especially anaerobically, indicating other limitations of xylose metabolism than just the redox balancing *(23)*.

We have previously carried out a metabolic flux analysis of xylose-utilizing *S. cerevisiae* grown aerobically and anaerobically in chemostat cultures on glucose or on xylose as the main carbon source *(24)*. The strain was constructed by introducing the XR- and XDH-encoding genes from the yeast *Pichia stipitis* and, further, by overexpressing the endogenous XK-encoding gene of *S. cerevisiae*. The aerobic and anaerobic phases of the cultures were studied by comparative two-dimensional electrophoresis (2-DE) gel analysis of soluble proteins *(25)*. In aerobic and anaerobic steady-state samples, 22 protein spots that responded to the change in the carbon source were identified.

In this article, we describe the use of DNA microarrays to analyze the samples derived from the aerobic phase of the same chemostat cultures studied by the 2-DE gel analysis. Present data confirm the downregulation of the citric acid cycle and upregulation of reactions balancing the cellular redox state, both observed in our metabolic flux and 2-DE gel studies. In addition, we present evidence that at a transcriptional level, xylose is not able to repress a starvation response, very similar to that reported during the acid-alkaline transition of growing yeast colonies *(26)*. Further, xylose seems neither a repressive nor a derepressive carbon source in *S. cerevisiae*, resulting in a mixed gene expression profile on this pentose sugar.

Materials and Methods

Yeast Strains

The genetically modified *S. cerevisiae* strain H2490 *(24)* based on the strain CEN.PK2 (*MAT*α, *leu2-3/112*, *ura3-52*, *trp1-289*, *his3*Δ*1*, *MAL2-8*^{c}, *SUC*2) *(27)* was used for the chemostat cultures. The strain H2490 contains the genes *XYL1* and *XYL2* of *P. stipitis* encoding XR and XDH, respectively, chromosomally integrated into the *URA3* locus. *XYL1* is expressed under the *PGK1* promoter and *XYL2* under the modified *ADH1* promoter *(28)*. In addition, the strain contains its endogenous XK-encoding gene (*XKS1*) between the modified *ADH1* promoter and *ADH1* terminator on the multicopy plasmid YEplac195 (uracil selection), and the multicopy plasmid YEplac181 (leucine selection) *(29)* with the *PGK1* promoter and terminator expression cassette with no insert.

Chemostat Cultures

The chemostat cultivations fed with yeast nitrogen base without amino acids (Difco, Detroit, MI) supplemented with 0.5 mL/L of silicone antifoam (AnalaR, BDH, Poole, UK) and either 10 g/L of glucose or 27 g/L of xylose and 3 g/L of glucose were carried out at 30°C as described previously *(24)* and are called glucose culture and xylose culture, respectively. The small amount of glucose in the feed of the xylose culture enabled the chemostat cultures on xylose. Reference *24* also describes in detail the gas analysis and determination of the culture's dry weight. Both fermentations were started as aerobic batch cultures with a working volume of 800 mL in 1.8-L Chemap

CMF fermentors (Chemap AG, Volketswil, Switzerland). To attain a dilution rate (D) of 0.05 h^{-1}, the feed of the medium was started when the carbon dioxide level in the batch cultures started to decrease. Before harvesting yeast for transcriptional analysis, the cultures were maintained for 7.5 residence times under aerobic conditions to obtain a metabolic steady state. The results presented here are from one culture each on glucose and xylose.

RNA Extraction

Yeast for transcriptional analysis was harvested from the aerobic steady states of glucose and xylose chemostat cultures by centrifuging 15-mL samples (1250*g* for 2 min at 20°C). The pellets were immediately frozen by liquid nitrogen and stored at –70°C. Frozen pellets were divided into smaller batches (six individual RNA extractions from both glucose- and xylose-grown cells were carried out) and broken by glass beads in Trizol reagent (Gibco-BRL, Life Technologies, Gaithersburg, MD). After extraction, RNA was precipitated by isopropyl alcohol, and the RNA pellet was rinsed with 80% (v/v) ethanol and resuspended in RNase-free water.

Yeast Gene Filter Hybridizations

[^{33}P]CTP-labeled cDNA was synthesized from each RNA preparation as follows: 2 µg of total RNA and 2 µg of oligo(dT) (10–20mer mixture, ResGen™; Invitrogen, Carlsbad, CA) were mixed with 8 µL of water, incubated at 70°C for 10 min, chilled on ice, and reverse transcribed with Superscript II (Gibco-BRL, Life Technologies) in the presence of [^{33}P]CTP (Amersham Pharmacia Biotech, Uppsala, Sweden) according to the protocol of ResGen. The cDNA was purified by passage through a Bio-Spin 6 chromatography column (Bio-Rad, Hercules, CA). Yeast Gene Filters I and II (ResGen) were prehybridized at 42°C for 4 h in a single hybridization tube with 5 mL of MicroHyb (ResGen) solution containing 5 µg of poly(dA) (ResGen). The purified cDNA was denatured for 5 min at 95°C and added to 5 mL of fresh prehybridization mixture. Hybridization was carried out for 18 h at 42°C in a roller oven (Hybaid, Heidelberg, Germany). Afterward, hybridization filters were washed according to the protocol of ResGen and exposed to a phosphor screen for 24 h. The phosphor screens were scanned at a resolution of 50 µm on a Typhoon instrument (Molecular Dynamics). Filters were stripped with boiling 0.5% sodium dodecyl sulfate, which was poured over the filters and allowed to cool for 15 min. To ensure stripping efficiency, the filters were re-exposed to a phosphor screen and the residual signal was measured from selected spots with the most intense signal. One wash was enough to bring the residual signal below 3% of the hybridization signal. Two pairs (1 and 2) of Gene Filters I and II were used for glucose vs xylose comparisons. In both cases, each filter pair was hybridized with cDNA prepared from both glucose- and xylose-grown cells (e.g., filter pair 1 was hybridized three times with xylose samples and three times with glucose samples), to minimize bias in the results owing to possible differ-

ences between filters. Six separate array analyses from individually prepared cDNAs from both glucose- and xylose-grown cells were carried out.

Microarray Analysis

The analysis cycle (RNA extraction, cDNA synthesis, and hybridization onto Yeast Gene Filters [ResGen]) was repeated six times each for the cells collected from the xylose and glucose chemostat cultures. Yeast Gene Filters contain 6144 polymerase chain reaction (PCR) products bound to two nylon filters designated I and II. The filters lack about 400 open reading frame (ORF) sequences mainly from chromosome 16. The images produced by the Typhoon instrument were imported to ArrayVision software (Imaging Research, Ontario, Canada) that was used for quantification of spot intensities. Normalization between sets of filters was based on the average signal intensities of control DNA spots on individual filters. Statistically significant changes in transcript abundance were obtained by importing normalized and background-reduced signal intensity values from each replicate hybridization into ArrayStat software (Imaging Research). In the analysis, data were log transformed, and the average log signal intensities for each gene were plotted on the *x*-axis while the corresponding standard deviations were plotted along the *y*-axis. The random error for each gene was calculated by a fitted curve that was used to estimate the relevant error for each gene *(30)*. Before a further statistical assessment of the microarray data, some data points were discarded from the analysis. These data points were outliers based on the data from replica hybridizations. The percentage of removed data points was 2.7 and 2.2% of all data points (36,864) within the six replicate hybridizations from aerobic glucose and xylose, respectively. In addition, some ORFs were excluded from the analysis because the signal from the replicate hybridizations was not sufficiently reproducible. After removing the outliers, the data were normalized by median across the two conditions studied, and the false discovery rate *(31)* with nominal α 0.05 was used as the false-positive error correction method. As a result, the responses between xylose and glucose were sorted to be significant or nonsignificant.

Promoter Analysis

Promoter analyses were carried out using Regulatory Sequence Analysis Tools at http://embnet.cifn.unam.mx/~jvanheld/rsa-tools/. Occurrences of known regulatory sequence patterns were searched for from promoter regions (up to 800 bp upstream of the coding region) of genes that were statistically significantly induced and downregulated by xylose.

Northern Analysis

The same six RNA preparations from both glucose and xylose cells that were used for cDNA synthesis were also used for Northern analysis of selected genes. Probes were prepared by PCR amplification of specific ORFs

from genomic DNA of the CEN.PK2 strain. The PCR fragments obtained were labeled with [α^{32}P]dCTP (Amersham Pharmacia Biotech) using a Hexalabel Plus™ DNA labeling kit (Fermentas, Manover, Maryland). Standard procedures for RNA blot hybridizations were followed *(32)*. Northern blot filters were scanned at 100-µm resolution using the Typhoon instrument, and signal intensities were quantified using ImageQuaNT software (Amersham Pharmacia Biotech). The measured values were normalized using the amount of *ACT1* mRNA as the control for each sample.

Results

The recombinant xylose-utilizing *S. cerevisiae* yeast was studied in chemostat cultures *(24)*. One chemostat was run with 10 g/L of glucose (glucose culture) and the other with 3 g/L of glucose + 27 g/L of xylose (xylose culture). To keep the growth rates identical, thus avoiding growth rate-dependent changes in the gene expression pattern, a dilution rate (D) of 0.05 h^{-1} was used in both cultures. Glucose was added (10% of total sugar) to the latter culture, because even the best recombinant xylose-utilizing *S. cerevisiae* strains have very low growth rates on sole xylose *(9,10,22,33)*. The residual glucose remained below the detection limit (0.06 g/L; <0.4 m*M*) throughout both the glucose and xylose culture, allowing us the assumption that yeast in the two cultures was in a glucose-derepressed state (*see* ref. *34*, and references therein).

Next we present the transcriptome analysis of cells collected from the aerobic steady states of glucose and xylose culture. Specific carbon utilization rates (C-mmol/[g-cell·h]) of glucose and xylose; oxygen consumption and production of biomass, xylitol, glycerol, acetate, and ethanol; as well as yields (C-mol/C-mol) over total carbon utilized have been reported previously *(24)*.

Statistical Analysis of Transcriptome Data

When yeast cells were metabolizing xylose, the expression level of 225 ORFs was altered in comparison to the glucose culture. At a confidence level of 95%, 125 of the responding genes were upregulated in the xylose chemostat culture (Supplemental Table 1), whereas 100 genes were downregulated (Supplemental Table 2). The differentially expressed genes were classified into functional categories to identify the biologic processes affected by aerobic xylose metabolism using the Medical Interactive Process System (MIPS) database. The results shown in Supplemental Tables 1 and 2 and in Fig. 2 are discussed in more detail in the following sections. Statistically significant changes in the transcript levels between the xylose and glucose samples were calculated by ArrayStat software *(30)*. The number of ORFs detected and included in the statistical analysis was 5500 (90% of the ORFs of *S. cerevisiae*).

The results of the statistical analysis were evaluated by Northern blotting analysis to verify independently changes for transcripts with different

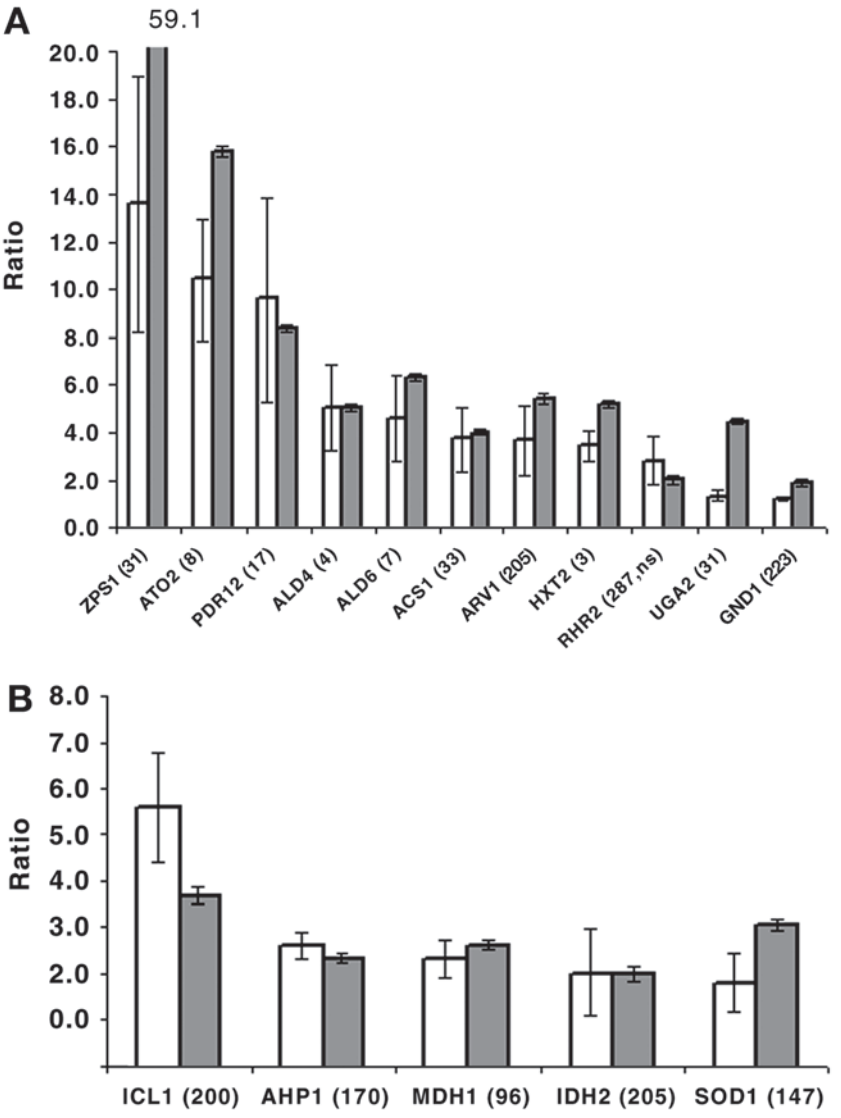

Fig. 1. Expression ratios of selected transcripts that were more abundant on **(A)** xylose or on **(B)** glucose were measured from Northern blots (□) and yeast gene arrays (■). The expression ratios of transcripts measured by Northern blots were calculated as an average from six individual RNA preparations. The expression ratios of transcripts measured by arrays were ranked to be significant and nonsignificant by *p* value obtained from a statistical test (*see* Results). The position in the significance ranking (1–225 were significant) is indicated after the gene names.

expression levels and with different significance ranking in the data analysis. The transcript ratios obtained by arrays on the two carbon sources studied were compared with the ratios obtained by the Northern hybridizations (Fig. 1). The Northern hybridization data of the selected 16 ORFs agreed well with the microarray data also when the change between the

glucose and xylose samples was not ranked statistically significant (*see RHR2* in Fig. 1A). Generally (except for two cases; *see ZPS1* and *UGA2* in Fig. 1A), the differences between the expression ratios obtained by either the arrays or the Northern blots were less than twofold. This shows the consistency of quantification between the arrays and Northern blots, and also the validity of the statistical analysis used.

Genes Encoding Activities of Central Carbon Pathways Have Altered Expression Profiles on Xylose

Comparison of yeast cells on xylose and glucose revealed significant differences in expression levels among genes encoding enzymes involved in the utilization of carbon compounds. In this functional group, 24 genes were downregulated and 9 genes were upregulated on xylose. In the oxidative part of PPP, *GND1*, encoding 6-phosphogluconate dehydrogenase, which catalyzes the second NADPH-producing step, had higher transcript levels on xylose (Fig. 2). However, the expression of *ZWF1* (encoding glucose 6-phosphate dehydrogenase; the first NADPH-producing step) and *SOL4* (encoding 6-phosphogluconolactonase) was slightly decreased (Fig. 2). Also notable is the two- to threefold lower expression of genes encoding malate dehydrogenase (Mdh1p), 2-oxoglutarate dehydrogenase isoenzymes Kgd1 and Kgd2p, isocitrate dehydrogenase (Idh2p), and fumarate hydratase (Fum1p) alike *ICL1* encoding isocitrate lyase, an enzyme of the glyoxylate cycle (Fig. 2). The observed transcript profiles of genes encoding activities of the PPP, tricarboxylic acid, and glyoxylate cycle correlate well with our earlier flux and proteome studies of the same cultivations *(24,25)*.

Furthermore, *PCK1*, encoding phosphoenolpyruvate carboxykinase, and *HXK1*, encoding hexokinase isoenzyme 1, had a lower expression level on xylose. Both of these genes normally have the highest expression during growth on carbon sources other than glucose *(35)* (Fig. 2). In acetate and acetyl-CoA metabolism, genes downregulated on xylose included *ALD2* and *ALD3*, encoding isoenzymes of cytosolic acetaldehyde dehydrogenases, and *ACH1*, encoding acetyl-CoA hydrolase (Fig. 2). Yet, the genes encoding the cytosolic (*ALD6*) and mitochondrial (*ALD4*) isoforms of acetaldehyde dehydrogenases had more than fivefold higher expression levels on xylose, concomitant with a fourfold higher expression of *ACS1*, encoding acetyl-CoA synthase (Fig. 2).

A Starvation Response Is Observed in Cells Metabolizing Xylose

The *ATO1*, *ATO2*, and *ATO3* genes were upregulated in the xylose culture (Table 1, Fig. 2). According to Palková et al. *(26)*, *ATO1-3* genes encode transporters of the YaaH family in *S. cerevisiae* and are directly involved in the excretion of ammonia from the cells during the acid-to-alkali transition phase that occurs in growing yeast colonies. Excretion of

ammonia is related to successful adaptation and survival under starvation conditions or entry into the stationary phase. It also contributes to a decrease in or an escape from the general stress response of the cells. Overall, changes in the expression of 33 genes (underlined in Tables 1 and 2) between the xylose and glucose cultures in the present study correlated qualitatively with changes observed by Palková et al. *(26)* with one exception: *CTR1* encoding a high-affinity copper transporter was present in both data sets but had increased expression on xylose, whereas it had decreased expression toward the alkali growth phase of yeast colonies. The changes that showed a relationship included the upregulation of *ALD4*, *ACS1*, *ICL2*, *ERG6* (encoding sterol methyltransferase), and *ERG25* (encoding methyl sterol oxidase), and of genes encoding zinc and phosphate transporters *ZRT1*, and *PHO84* and *PHO89*, respectively, and the downregulation of *ICL1*, *ACH1*, *IDH2*, *KGD1*, and *FUM1*. A significant number of these genes encode enzymes of the tricarboxylic acid cycle and acetyl-CoA metabolism. In summary, a large proportion, approx 15%, of the genes showing an altered expression profile on xylose compared to glucose seems to be involved in a starvation response.

Genes Encoding Activities for Carbon Scavenging Are Upregulated on Xylose

ICL2, a homolog of *ICL1* that encodes 2-methylisocitrate lyase of the mitochondrial matrix, had a fivefold increase in expression in the xylose culture (Table 1). The enzyme converts 2-methylisocitrate into pyruvate and succinate in the 2-methylcitrate cycle, a part of propionyl-CoA metabolism. The physiologic function of this cycle is not fully understood in *S. cerevisiae*, but it is presently believed that the cycle has a role in scavenging carbon skeletons from certain amino acids *(36)*. Transcription of *ARO10* and *AAD14* genes was also upregulated in the xylose culture 4- and 28-fold, respectively (Table 1). *ARO10* encodes a phenylpyruvate decarboxylase that is involved in the catabolism of leucine and phenylalanine to aldehyde *(37)*, and *AAD14* encodes an enzyme possibly able to reduce the aldehydes formed *(38,39)*.

The Biosynthesis of Lipids and Isoprenoids Is Enhanced on Xylose

The synthesis of sterols comprises more than 20 distinct reactions in two subsequent pathways. The mevalonate pathway from acetyl-CoA leads to farnesyl pyrophosphate, an important intermediate as a starting point for several different pathways *(40)*. On xylose, 5 of the 12 steps of the second pathway leading from farnesyl pyrophosphate to ergosterol were upregulated at the transcriptional level (Supplemental Fig. 1). In addition, a higher amount of transcripts for Arv1p was detected (Fig. 2). Arv1p has been suggested to play a role both in the regulation of sterol and sphingolipid metabolism and in the trafficking of lipids *(41)*.

PM
HXT2 5.2
MAL11 -2.9
MAL31 -6
ZRT1 15.6
ZRT2 2.8
ZRT3 2.2
CTR1 10.5
PHO89 3.7
PHO84 3.2
PHO88 2.7
FTH1 -5.5
FTR1 -2.1
FET3 -3
JEN1 3
PDR12 8.4
GAP1 3.7
GUP2 13.7
ENA1 2.5
ATO1 11.7
ATO2 15.8
ATO3 3.8
NH4+
ENB1 -2.9
FET6 -3.1
ARV1 5.4
NHX1 -3.6
Legend
Increased > 2-fold and significant
Increased > 2 fold but not significant
Decreased < -2-fold and significant
Decreased < -2 fold but not significant
Signif= n/a
No criteria met
Not found
D-Xylose
NAD(P)H
XR
NAD(P)+
Xylitol
NAD+
XDH
NADH
Xylulose
ATP
XKS1 1.4
R5P
RPI1 1.2
Ru5P
RPE1 1.2
NADPH+CO2
GND1 1.9
GND2 1.2
6-PGlnate
NADP+
SOL4 -6
6-PGl
ZWF1 -2
NADP+ NADPH+H+
Xu5P
TKL1 1.5
TKL2 1
S7P+G3P
TAL1 1.9
TAL2 -2.5
E4P+F6P
F6P+Ga-3-P
GSY2 1.4
GSY1
GLG1 -1.9
GLG2 2.1
GLC3 -4
Glycogen
GDB1
GPH1
UDP-Glu
UGP1 -4
Glu-1-P
PGM1 2.2
PGM2 -12
Glu-6-P
PGI1 1
Fru-6-P
ATP
PFK1 -1.5
PFK2 1.1
ADP
Fru-1,6-P
FBA1 2
FBP1
DHAP
TPI1 1.5
Ga-3-P
NAD+
TDH1 1.1
TDH2 -1.2
TDH3 -1
NADH
1,3-Bpg
PGK1 1
3-Pg
GPM1 1.6
GPM2 4.2
GPM3 12.1
TSL1 -11
TPS1 -3.3
TPS2 -2.1
TPS3 -1.6
Trehalose
NTH1
NTH2 1.2
ATH1 -1.7
Glucose
HXK1 -2.4
HXK2 -1.1
GLK1 -1.9
ATP
ADP
NADH
GPD1 -1.6
GPD2 -1
NAD+
Glycerol-3-P
GPP1 2.1
GPP2 -1.5
Glycerol

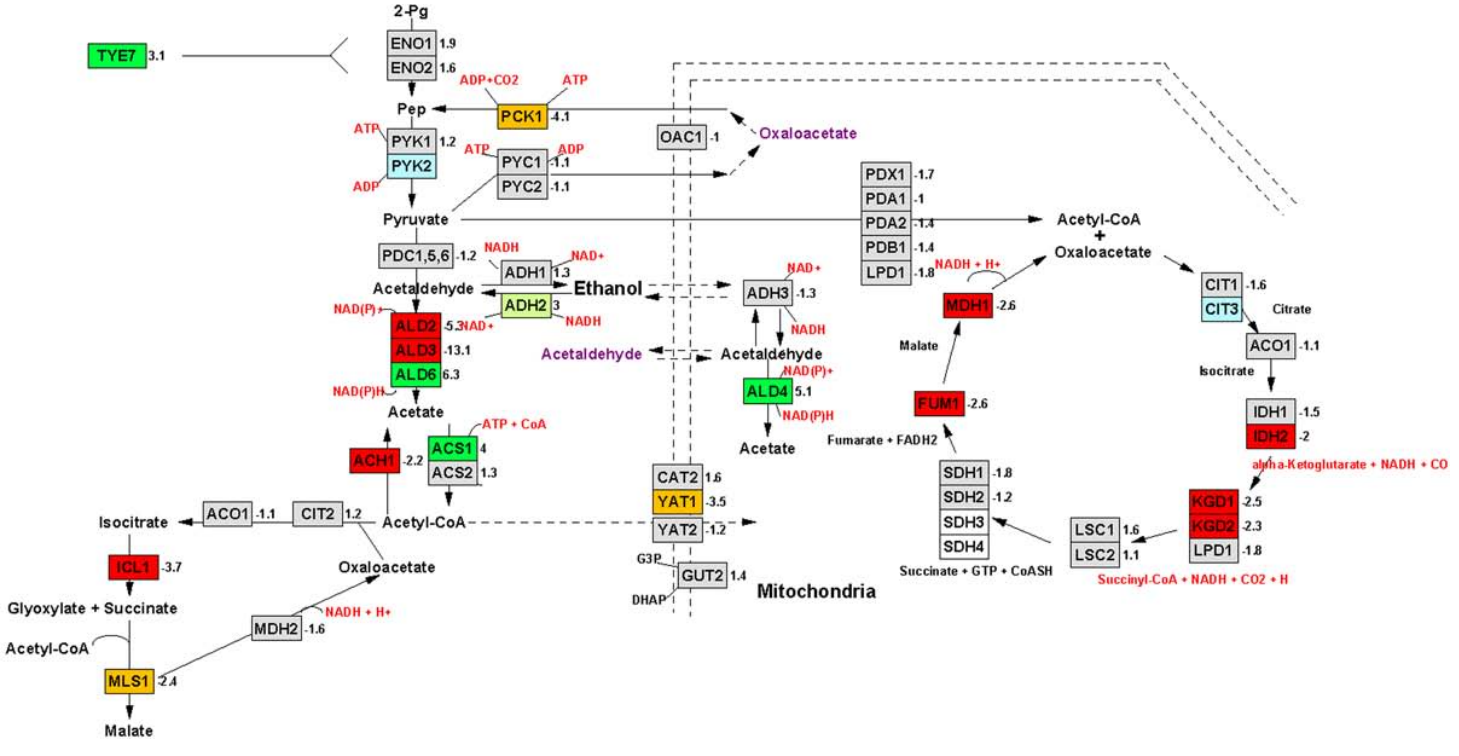

Fig. 2. Schematic representation of central carbon pathways in yeast. Selected mitochondrial functions and plasma membrane transporters affected in this study are also shown. Expression ratios are marked next to the genes; positive values indicate upregulation and negative values downregulation on xylose. Dark green shows statistically significantly increased expression levels in xylose culture compared to glucose, and light green more than twofold increased expression that, however, was not statistically significant. Red indicates statistically significantly decreased expression levels on xylose and orange more than twofold but not statistically significantly decreased levels. Expression levels of genes marked in gray did not change. Blue indicates that no signal was detected and white that the ORF was absent from the array. The figures were drawn using GenMAPP software (www.genmapp.org) *(64)*.

Table 1
Genes With Increased Expression Level in Xylose Compared to Glucose Culture[a]

ORF ID	Gene	Fold change	Description
			Amino acid metabolism
YBR006w	*UGA2*	4.4	Succinate semialdehyde dehydrogenase
			Classification not yet clear
YDL214c	*PRR2*	2.9	Strong similarity to putative protein kinase Npr1
YER089c	*PTC2*	20.3	Protein serine/threonine phosphatase of PP2C family
			C-compound and carbohydrate utilization
YNL331c	*AAD14*	27.9	Strong similarity to aryl-alcohol reductase
YAL054c	*ACS1*	4.0	Acetyl-CoA synthetase
YOR374w	*ALD4*	5.1	Aldehyde dehydrogenase, mitochondrial
YDR380w	*ARO10*	4.4	Phenylpyruvate decarboxylase
YBR020w	*GAL1*	2.5	Galactokinase
YPR006c	*ICL2*	4.9	2-Methylisocitrate lyase
			Cell cycle and differentiation
YNL307c	*MCK1*	22.3	ser/thr/tyr protein kinase
YER044c-a	*MEI4*	52.6	Meiosis-specific protein
			Control of cellular organization
YKL096w-a	*CWP2*	1.9	Cell wall mannoprotein
YNR030w	*ECM39*	3.2	Involved in cell wall biogenesis and architecture
YLR425w	*TUS1*	3.4	TOR Unique function Suppressor; exchange factor for Rho1p, cell wall integrity
			Detoxification
YDR256c	*CTA1*	4.3	Catalase A, peroxisomal
			Homeostasis of ions
YLR433c	*CNA1*	9.3	Calcineurin B, catalytic subunit
YPR124w	*CTR1*	10.5	Copper transport protein
YEL027w	*CUP5*	13.4	H^+-ATPase V0 domain 17-kDa subunit, vacuolar
YMR038c	*LYS7*	3.5	Copper chaperone for superoxide dismutase Sod1p

YML123c	*PHO84*	3.2	High-affinity inorganic phosphate/H^+ symporter
YBR296c	*PHO89*	3.7	Na^+-coupled phosphate transport protein, high affinity
YLR447c	*VMA6*	3.7	H^+-ATPase V0 domain 36-kDa subunit, vacuolar
YGL255w	*ZRT1*	15.6	High-affinity zinc transport protein
			Lipid fat and isoprenoid metabolism
YGR060w	*ERG25*	3.3	C-4 Sterol methyl oxidase
YML008c	*ERG6*	2.4	*S*-Adenosyl-methionine δ-24-sterol-*c*-methyltransferase
YKR009c	*FOX2*	2.1	Hydratase-dehydrogenase-epimerase, peroxisomal
			Metabolism of vitamins, cofactors and prosthetic groups
YOL151w	*GRE2*	3.9	Similarity to plant dihydroflavonol-4-reductases
			Regulation of C-compound and carbohydrate metabolism
YOR344c	*TYE7*	3.1	Basic helix-loop-helix transcription factor, needed for maximal expression of enolase
YFL052w		5.4	Strong similarity to Mal63p, YPR196w, and Mal13p
			Stress response and protein folding
YLR417w	*VPS36*	24.9	Defective in vacuolar protein sorting
			Transcription
YPR057w	*BRR1*	14.1	Involved in snRNP biogenesis
YER159c	*BUR6*	2.4	Functional homolog of human NC2α, transcriptional regulator
YPR025c	*CCL1*	23.7	TFIIH subunit (transcription initiation factor), cyclin C component
YLR433c	*CNA1*	9.3	Possible involvement of calcineurin B, catalytic subunit, in regulation of some ion pumps
YBR020w	*GAL1*	2.5	Galactokinase
YPR068c	*HOS1*	11.7	Histone deacetylase
YPR070w	*MED1*	22.3	Component of RNA polymerase II holoenzyme and mediator subcomplex
YBR193c	*MED8*	2.8	RNA polymerase II transcriptional regulation mediator
YMR287c	*MSU1*	3.3	3'-5' Exonuclease for RNA 3' ss-tail, mitochondrial
YBR066c	*NRG2*	3.4	Weak similarity to *Aspergillus niger* carbon catabolite repressor protein, interacts with Snf1p
YHR206w	*SKN7*	2.4	Transcription factor with similarity to Hsf1p (osmotic and oxidative stress)
YPR086w	*SUA7*	6.2	TFIIB subunit (transcription initiation factor), factor E
YKL058w	*TOA2*	2.0	TFIIA subunit (transcription initiation factor), 13.5 kDa

(continued)

Table 1 *(continued)*

ORF ID	Gene	Fold change	Description
YOR344c	*TYE7*	3.1	Basic helix-loop-helix transcription factor
YJL056c	*ZAP1*	3.0	Metalloregulatory protein involved in zinc-responsive transcriptional regulation
YFL052w		5.4	Strong similarity to Mal63p, YPR196w, and Mal13p
YER130c		2.4	Similarity to Msn2p and weak similarity to Msn4p
			Transport facilitation
YCR010c	*ATO1*	11.7	Member of YaaH family of putative transporters
YNR002c	*ATO2*	15.8	Member of YaaH family of putative transporters
YDR384c	*ATO3*	3.8	Member of YaaH family of putative transporters
			Unclassified
YIL057c		11.6	Strong similarity to unknown protein YER067w
YOL101c		3.6	Similarity to YOL002c involved in PHO signaling pathway
YOL154w	*ZPS1*	59.1	Putative GPI-anchored protein, transcription induced under low zinc and alkaline pH
YML006c	*GIS4*	50.3	Suppressor of Gig3 cyclin-dependent protein kinase
YMR316c-a		36.1	Unknown function
YNL028w		30.2	Unknown function
YPL073c		110.8	Unknown function
YPR038w		132.1	Unknown function

[a]The genes with a qualitative correlation with the transcriptional changes observed by Palková et al. *(26)* during the transition of yeast colonies from the acid-to-ammonia secretion phase are underlined. ATPase, adenosine triphosphatase.

Genes Encoding Various Transporters Respond to Xylose as a Carbon Source

Transcripts for genes encoding several zinc and phosphate transporters were more abundant on xylose than on glucose, whereas, in turn, genes encoding iron permeases and the endosomal/prevacuolar Na^+/K^+ exchanger Nhx1p were attenuated. In addition, an increased expression level was detected for *HXT2* encoding one of the several hexose transporters in yeast, for *GAP1* encoding a general amino acid permease, and for *JEN1* encoding a carboxylic acid transporter (Fig. 2, Tables 1 and 2).

Genes Encoding Various Transcription Factors Have Altered Expression Profiles on Xylose

At least 17 genes closely involved in transcription were upregulated 2- to 54-fold on xylose (Table 1), whereas 5 genes were downregulated 2- to 6-fold (Table 2). The most interesting of these genes were related to the regulation of carbon metabolism and the environmental stress response. Further, the occurrence of known regulatory sequence patterns for several transcription factors was searched from promoter regions (800 bp upstream of the coding region) of all statistically significant xylose-responding genes (*see* Supplemental Table 3).

The gene encoding galactokinase (*GAL1*) had higher transcript levels on xylose, as did the genes encoding transcription factors Med1p, Bur6p, and Nrg2p, known to be regulating the transcription of *GAL* genes *(42,43)* (Table 1). *BUR6* is also putatively linked to the regulation of environmental stress response *(44)*. Transcripts of *NRG2* were shown to be elevated in response to zinc limitation and alkaline pH *(45)*, and its promoter region has a potential binding site for the zinc-responsive transcription factor encoded by *ZAP1 (46)*. Other targets of Zap1p with increased expression on xylose were genes encoding zinc transporters (Fig. 2) and *GRE2* encoding a protein with oxidoreductase activity (Table 1). The expression of *ZAP1* correlated with the expression of its target genes; *ZAP1* was upregulated threefold, and, correspondingly, 6% of the genes upregulated and 3% of the genes downregulated on xylose had a binding site for this transcription factor.

Furthermore, *SKN7* had a twofold higher expression level in the xylose culture. A branch of the mitogen-activated protein kinase pathway involving Skn7p as the regulator is activated in response to hypoosmotic stress *(47)* and is involved in controlling cell wall integrity *(48)* and cell cycle *(49)*. Via a different activation mechanism Skn7p plays a role also in the oxidative stress resistance *(50)*. However, only 14% of the promoters of the genes significantly upregulated on xylose had stress-responsive element binding sites for the transcription factors Msn2p/Msn4p, involved in the induction of general stress response in the cells, whereas 45% of the promoter regions of the downregulated genes had these binding sites although neither *MSN2* nor *MSN4* had altered expression levels. However, *YER130c* encoding a protein with similarity to Msn2/4p was upregulated (Table 1).

Table 2
Genes with Decreased Expression Level on Xylose Compared to Glucose Culture[a]

ORF ID	Gene	Fold change	Description
			Cell cycle and differentiation
YJL079c	*PRY1*	2.2	Strong similarity to plant PR-1 class of pathogen-related proteins
			C-compound and carbohydrate utilization
YBL015w	*ACH1*	2.2	Acetyl-CoA hydrolase
YPL262w	*FUM1*	2.6	Fumarate hydratase
YEL011w	*GLC3*	4.0	1,4-Glucan-branching enzyme (glycogen-branching enzyme)
YGR032w	*GSC2*	2.2	1,3-β-D-glucan synthase subunit
YER065c	*ICL1*	3.7	Isocitrate lyase
YOR136w	*IDH2*	2.0	Isocitrate dehydrogenase (NAD^+) subunit 2, mitochondrial
YIL125w	*KGD1*	2.5	2-Oxoglutarate dehydrogenase complex E1 component
YGR292w	*MAL12*	2.2	α-D-Glucosidase of MAL1 locus
YBR299w	*MAL32*	4.0	α-D-Glucosidase
YIL045w	*PIG2*	7.6	Protein interacting with glycogen synthase Gsy2p
YBR126c	*TPS1*	3.3	α,α-Trehalose-phosphate synthase, 56-kDa subunit
YDR074w	*TPS2*	2.1	α,α-Trehalose-phosphate synthase, 102-kDa subunit
YML100w	*TSL1*	11.0	α,α-Trehalose-phosphate synthase, 123-kDa subunit
			Control of cellular organization
YER150w	*SPI1*	5.1	Stationary Phase Induced protein
			Detoxification
YJR104c	*SOD1*	3.1	Copper-zinc superoxide dismutase
YHR008c	*SOD2*	2.9	Superoxide dismutase (Mn) precursor, mitochondrial
			Oxidation of fatty acids
YNL202w	*SPS19*	44.2	Peroxisomal 2,4-dienoyl-CoA reductase
			Stress response and protein folding
YDR033w	*MRH1*	2.6	Membrane protein related to Hsp30p
YNL160w	*YGP1*	5.6	Secreted glycoprotein

YGR234w	*YHB1*	3.0	Flavohemoglobin
YBR054w	*YRO2*	3.0	Strong similarity to Hsp30 heat-shock protein Yro1p
			Transcription
YKL043w	*PHD1*	2.0	Transcription factor
YHR056c	*RSC30*	6.3	RSC complex component
YKR092c	*SRP40*	2.1	Suppressor of mutant AC40 of RNA polymerase I and III
YDL048c	*STP4*	4.8	Involved in pre-tRNA splicing and in uptake of branched-chain amino acids
YLR136c	*TIS11*	3.0	tRNA-specific adenosine deaminase 3
			Transport facilitation
YKL198c	*PTK1*	24.2	Polyamine transport-enhancing protein
			Unclassified
YOR382w	*FIT2*	2.8	Hypothetical protein
YER067w		18.0	Strong similarity to hypothetical protein YIL057c
YKL044w		2.5	Hypothetical protein
YLR456w		24.4	Strong similarity to hypothetical ORF YPR172w
YMR172c-a		41.0	Questionable ORF

[a]The genes with a qualitative correlation with the transcriptional changes observed by Palková et al. *(26)* during the transition of yeast colonies from the acid-to-ammonia secretion phase are underlined.

Linked to the regulation of carbon utilization, *TYE7* encoding an E-box DNA-binding protein that is a multicopy suppressor of *gcr2* mutants had threefold more transcripts on xylose compared to glucose (Table 1, Fig. 2). Gcr2p acts with Gcr1p to mediate a high level of glycolytic gene expression *(51)*. However, overexpression of *TYE7* in our recombinant xylose-metabolizing *S. cerevisiae* did not result in improved performance on xylose (our unpublished results).

Furthermore, 18% of the promoter regions of the upregulated genes on xylose had at least two binding sites for the transcription factor Adr1p, whereas only 9% of the promoter regions of the downregulated genes fell into this class. Moreover, neither Mig1p nor Pho4p whose binding sites were slightly overpresented in the promoter regions of genes upregulated on xylose (11 vs 9% and 2 vs 0%, respectively) had altered expression profiles on this sugar. However, several genes encoding phosphate transporters induced by Pho4p were upregulated on xylose.

Additionally, *YFL052w*, with similarity to, e.g., Malx3p transcription factors of *MAL* loci, had fivefold higher transcript levels on xylose. *YFL052w* encodes a zinc-finger protein, and deletion of this gene impairs growth on nonfermentable carbon sources *(52)*. However, there was no difference in abundance of Cat8p (involved in derepression of the genes encoding gluconeogenic enzymes) binding sites in the promoter regions of xylose-affected genes.

Discussion

Recently, DNA microarray studies with xylose-metabolizing recombinant *S. cerevisiae* have been reported, but contrary to the present study, the analyses either were carried out in shake-flask cultures with a batch mode *(53,54)*, or they compared a xylose-utilizing yeast strain with a mutated strain with improved xylose metabolism *(55,56)*. We report herein on a continuous chemostat study of a nonmutated xylose-fermenting *S. cerevisiae* strain. Compared with batch cultures, continuous cultures enable the control of, e.g., growth rates, cell densities, and substrate concentrations. Thus, comparative studies with different carbon sources are possible and growth rate-related phenomena can be excluded. The current recombinant xylose-utilizing *S. cerevisiae* strains have low growth rates even under aerobic conditions on sole xylose *(10,22)*. The lack of a feasible growth rate on this pentose sugar was the reasoning behind the setup of the xylose culture, in which we added 3 g/L of glucose (10% of the total carbon) to the feed of the xylose chemostat. As a result, in our chemostat cultivations of xylose as the main carbon source, the growth rates, cell densities, and residual glucose concentrations (<0.06 g/L; <0.4 m*M*) were comparable with those in the glucose chemostat. The extracellular glucose was below the critical repressing concentration (14 m*M*; *see* ref. *34* and references therein). As demonstrated, e.g., in a recent article by Daran-Lapujade et al. *(57)*, glucose repression does not occur in glucose-limited chemostat

cultures owing to the low residual glucose concentration. The main difference between the cultures was that on xylose only 70% of the carbon utilized was xylose, and there was residual xylose in the extracellular medium. Hence, in our setup we were able to assess whether the residual xylose is able to repress the genes encoding activities of gluconeogenesis, or glyoxylate and tricarboxylic acid cycles. Furthermore, 30% of the carbon utilized by the cells in the xylose culture was glucose. In term of fluxes, the glucose flux in the xylose culture (1.95 C-mmol/[g-cell·h]) was approx 27% of that in the glucose culture (7.22 C-mmol/[g-cell·h]). Thus, there is a difference in the glucose flux when the two cultures are compared. Elbing et al. *(58,59)*, among others, indicated a correlation between glucose consumption rate and glucose repression. When studied in a batch mode (external glucose of 15–25 g/L), the expression of gluconeogenic genes *FBP1* and *MDH2* was repressed to a lower extent, and the expression of *SUC2* encoding invertase was induced in a yeast strain with a lower glucose consumption rate *(59)*. However, in the present chemostat study, the level of *SUC2* (data not shown) and *FBP1* transcripts (Fig. 2) was comparable in the xylose and glucose culture, whereas genes encoding gluconeogenic and glyoxylate cycle enzymes (*ICL1*, *PCK1*, *MLS1*, and *MDH2*) exhibited lower expression levels in the xylose culture compared with the glucose culture (Fig. 2). If indeed the different glucose consumption rates in the two chemostat cultures resulted in a difference in the level of glucose derepression, the residual xylose must have masked this effect.

Effects of Cofactor Imbalance on Gene Expression on Xylose

The different cofactor preferences of XR and XDH are believed to disturb the cellular cofactor pools during xylose consumption. One of the objectives of the present study was to discover how the apparent redox imbalance affects the cellular metabolism. In light of recent results with xylose isomerase offering an excellent solution to overcome redox issues in xylose fermentation by recombinant *S. cerevisiae (21,22)*, this may seem superfluous. However, metabolic engineering efforts are likely to affect the cellular redox state in general, and the oxidoreductive xylose conversion offers a good model system to study it. Under aerobic xylose metabolism by the oxidoreductive pathway, the main challenge is the regeneration of NADPH. Indeed, on xylose several genes encoding oxidoreductases had higher transcript levels compared to glucose culture. We believe that this reflects a metabolic response that the cell takes to balance its redox state. Furthermore, metabolic flux analysis *(24)* indicated increased flux through the oxidative branch of the PPP in xylose chemostats. The upregulation of expression of *GND1* is consistent with this finding and may further relate to the increased NADPH demand owing to XR reaction. In addition, *ALD6* had higher expression on xylose, possibly facilitating NADPH regeneration by oxidation of acetaldehyde to acetate. The mitochondrial Ald4p, which also has increased transcript levels on xylose, participates in $NAD(P)^+$ reduction in mitochondria contributing to the pool of reduced

cofactors that may be exported to the cytosol by the ethanol-acetaldehyde shuttle *(60)*. On the other hand, we detected increased expression of several genes encoding the enzymes of the ergosterol biosynthetic pathway, which is highly NADPH consuming. A tentative explanation is that lack of NADPH leads to a low level of sterols, which, in turn, stimulates the expression of these genes. In summary, it seems that several metabolic reactions, either to regenerate the actual cofactors or to choose a more optimal reaction to conserve cofactors, are activated or attenuated to regain the cellular redox balance.

Tricarboxylic Acid and Glyoxylate Cycles Were Downregulated on Xylose

Overall, of the 22 xylose-responding proteins identified in the comparative 2-DE gel study *(25)* of the same culture samples, 9 responded qualitatively in a similar manner at the transcriptional level (Table 3). Additionally, the expression of seven other genes correlated with the 2-DE gel analysis, but the response was not statistically significant. Consistent with the present transcriptional analysis and the xylose flux study *(24)* of the same cultivation, we observed decreased protein concentrations on xylose in the tricarboxylic acid cycle. This response and, likewise, the decreased activity in the glyoxylate cycle and respiration may be owing to increased mitochondrial NADH concentrations during growth on xylose. We see consistent indications of NADH shuttling in the proteome *(25)* and the present transcript study as mitochondrial (Ald4p; *ALD4*) and cytosolic (Ald6p; *ALD6*) isoenzymes of acetaldehyde dehydrogenase were upregulated (Table 3). The more NADH is shuttled to mitochondria from the cytosol, the less tricarboxylic acid cycle activity is required. In addition, there is evidence that mitochondrial NADH inhibits the first reactions of the tricarboxylic acid cycle *(61)*. Because the tricarboxylic acid cycle and oxidative phosphorylation are joined in the succinate dehydrogenase complex, respiration also may get forcefully reduced, although there is abundant NADH available. Reduced respiration with respiratory quotient (RQ) 1.2 was demonstrated in the xylose flux study, and the RQ value increased further when the amount of additional glucose in the feed was decreased *(24)*. Glyoxylate cycle bypasses the NADH-producing reactions of isocitrate dehydrogenase and α-ketoglutarate dehydrogenase. However, on xylose the main genes of the glyoxylate cycle were downregulated (*ICL1*, *MLS1*) although the increased levels of *ACS1* transcripts point toward increased cytosolic acetyl-CoA concentrations (Fig. 2).

Starvation-Induced Genes on Xylose

Expression of *ATO1*, *ATO2*, and *ATO3* was found to increase in the ammonia secretion phase during the periodic transition of yeast colonies from acid to ammonia production *(26)*. According to Palková et al. *(26)*, Ato1–3 are involved in ammonia secretion by yeast cells in colonies.

Table 3
Proteome Responses on Xylose Compared to Glucose, and Their Correlation to Transcriptional Changes, Analyzed From Yeast Harvested at Same Time Point of Chemostat Cultures[a]

Gene	Proteome increase (↑) or decrease (↓)	Transcriptome upregulation (+) or downregulation (–)	Description
ALD6	↑	+6.3	Aldehyde dehydrogenase, cytosolic
ALD4	↑	+5.1	Aldehyde dehydrogenase, mitochondrial
CYB2	↑	+2.1	Lactate dehydrogenase cytochrome b2
FUM1	↓	–2.6	Fumarate hydratase
GCV1	↓	–3.0	Glycine decarboxylase, subunit T
HSP78	↓	–2.9	Heat-shock protein 78, member of clpb family of ATP-dependent proteases, mitochondrial
IDH2	↓	–2.0	Isocitrate dehydrogenase (NAD^+) subunit 2, mitochondrial
MDH1	↓	–2.6	Malate dehydrogenase precursor, mitochondrial
YHB1	↓	–3.0	Flavohemoglobin
ADH2	↑	+3.0 (ns, 281)	Alcohol dehydrogenase 2
GPP1	↑	+2.1 (ns, 289)	DL-Glycerol-3-phosphatase
ADO1	↓	+1.7 (ns, 495)	Adenosine kinase
ENO2	↑	+1.6 (ns, 582)	Enolase 2
GPD1	No change	–1.6 (ns, 775)	Glycerol-3-phosphate dehydrogenase
HSP26	↑	+1.7 (ns, 1121)	Heat-shock protein 26
IDH1	↓	–1.5 (ns, 1214)	Isocitrate dehydrogenase 1
ATP7	↓	–1.3 (ns, 2056)	ATP synthase d subunit
YMR315W	↑	+1.7 (ns, 2379)	Unknown function
SSE1	↑	–1.2 (ns, 2575)	Member of HSP70 family, highly homologous to Ssa1p and Sse2p
ADK1	↓	–1.3 (ns, 3114)	Adenylate kinase, cytosolic
LYS4	↑	+1.2 (ns, 4364)	Homoaconitase
PRX1	↓	Absent from the array	Thioredoxin peroxidase, mitochondrial

[a]A more detailed description of the proteome analysis has been published *(25)*. The position in the significance ranking in the transcriptional analysis is indicated for the nonsignificant changes (ns) (1–225 were significant and 226–6144 were nonsignificant changes). ATP, adenosine triphosphate.

The secreted ammonia is a starvation signal that directs growth of the colonies away from the neighboring colonies and toward more nutrient-rich areas on the plate. *ATO1–3* were strongly upregulated also on xylose in our study. Moreover, the expression of *ICL2* was increased, whereas genes encoding activities of the tricarboxylic acid cycle and the general stress response were downregulated both in our xylose-consuming cells and in the yeast colonies during the ammonia secretion phase. Altogether, expression profiles of 33 of 225 genes between the xylose and glucose cultures in our study correlated with changes observed by Palková et al. *(26)*. These results emphasize a neglected aspect of xylose metabolism by recombinant *S. cerevisiae*; in many ways, the yeast cell responds to xylose as though it were experiencing carbon starvation, and the presence of residual xylose is not enough to repress this response. We believe that this observation is of general importance in constructing xylose-metabolizing *S. cerevisiae* strains.

Is Xylose a Repressing or Derepressing Carbon Source?

Contrary to xylose batch cultivations by Jin et al. *(54)* in which glucose-repressed cells were compared with cells on xylose, upregulation of genes encoding primary gluconeogenic enzymes was not detected over glucose in our chemostat cultivations on xylose. Instead, our results lend support to those of Roca et al. *(14)*, who observed repression of the gene encoding invertase in both parental and *mig1*-deleted, xylose-utilizing yeast strains grown on a glucose-xylose mixture compared to glucose alone. Because the glucose level of their chemostat cultures was below a repressing concentration, they concluded that xylose itself is a repressing carbon source. The reason that Jin et al. *(54)* observed upregulation of genes encoding primary gluconeogenic enzymes in their xylose batch cultures may be that the cells produced ethanol to the medium. Thus, it is possible that in their setup the cells responded to ethanol by derepression and xylose was not able to repress the derepression.

Belinchón and Gancedo *(62)* studied the effect of different non-fermentable carbon sources including xylose on the repression of gluconeogenic enzymes. When a recombinant xylose-metabolizing *S. cerevisiae* strain was grown on glucose under repressing conditions and then incubated in a medium containing ethanol and xylose, xylose prevented the derepression by ethanol of fructose 1,6-bisphosphatase (Fbp1p) and isocitrate lyase (Icl1p). Furthermore, as the same strain was grown to exponential growth phase on different carbon sources, lower Fbp1p and Icl1p activities were detected on xylose, or on a mixture of ethanol and xylose, compared to the cells grown on ethanol alone. However, the activity levels of these two enzymes on xylose were still considerably higher, 20- to 30-fold, compared to glucose-grown cells, indicating that xylose was not able to fully repress these enzymes *(62)*. In addition, we have observed higher Icl1p and Fbp1p enzyme activities in xylose-grown cells compared with glucose-grown cells, lending further support to xylose not being recognized as a true repressing carbon source. However, xylose is not truly

derepressing either, because the Icl1p and Fbp1p enzyme activities were considerably higher on ethanol-grown than on xylose-grown cells *(33)*.

MED1, *MED8*, *BUR6*, and *NRG2* with higher expression on xylose than glucose encode transcription factors involved in the derepression of glucose-repressible genes. Moreover, many genes upregulated in the xylose culture and regulated by Adr1p significantly outnumbered the genes with a higher level of expression in the glucose culture. It was recently shown that the expression of 108 genes is decreased in the absence of Adr1p *(63)*. These genes are members of various functional classes, but the majority of them are related to the oxidation of different nonfermentable carbon sources and, further, to the generation of acetyl-CoA and NADH from these substrates.

When all the data are considered, the response to xylose at the transcriptional level seems unclear. In our studies, xylose appears as a weakly repressing carbon source, because the genes encoding primary gluconeogenic enzymes were downregulated compared to a glucose culture that was in a glucose-derepressed mode. On the other hand, xylose is not able to repress either the starvation response or a number of genes encoding activities to allow the cell to utilize alternative carbon sources. Identification of the signaling cascades that xylose activates or fails to activate in yeast cells will strongly influence the successful outcome of future metabolic engineering efforts at xylose fermentation.

Acknowledgments

We thank Ari Rantanen for indispensable help in the computational analysis of the gene expression data. We also acknowledge Mervi Toivari for helpful discussions and Pirjo Tähtinen for excellent technical assistance. Finally, we are grateful to John Londesborough for numerous suggestions on improving the manuscript. This work was financed by the Technology Agency of Finland (project no. Tekes 40416/01). This work is also part of the research program VTT Industrial Biotechnology (Academy of Finland; Finnish Center of Excellence program, 2000–2005, project no. 64330).

References

1. Jeffries, T. W. and Jin, Y.-S. (2004), *Appl. Microbiol. Biotechnol.* **63,** 495–509.
2. Ho, N. W., Chen, Z., and Brainard, A. P. (1998), *Appl. Environ. Microbiol.* **64,** 1852–1859.
3. Eliasson, A., Christensson, C., Wahlbom, C. F., and Hahn-Hägerdal, B. (2000), *Appl. Environ. Microbiol.* **66,** 3381–3386.
4. Toivari, M. H., Aristidou, A., Ruohonen, L., and Penttilä, M. (2001), *Metab. Eng.* **3,** 236–249.
5. Toivari, M. H., Salusjärvi, L., Ruohonen, L., and Penttilä, M. (2004), *Appl. Environ. Microbiol.* **70,** 3681–3686.
6. Eliasson, A., Hofmeyr, J. H., Pedler, S., and Hahn-Hägerdal, B. (2001), *Enzyme Microb. Technol.* **29,** 288–297.
7. Jin, Y. S., Ni, H., Laplaza, J. M., and Jeffries, T. W. (2003), *Appl. Environ. Microbiol.* **69,** 495–503.

8. Anderlund, M., Radström, P., and Hahn-Hägerdal, B. (2001), *Metab. Eng.* **3,** 226–235.
9. Wahlbom, C. F., van Zyl, W. H., Jonsson, L. J., and Hahn-Hägerdal, B. (2003), *FEMS Yeast Res.* **3,** 319–326.
10. Sonderegger, M. and Sauer, U. (2003), *Appl. Environ. Microbiol.* **69,** 1990–1998.
11. Walfridsson, M., Hallborn, J., Penttilä, M., Keränen, S., and Hahn-Hägerdal, B. (1995), *Appl. Environ. Microbiol.* **61,** 4184–4190.
12. Jeppsson, M., Johansson, B., Hahn-Hägerdal, B., and Gorwa-Grauslund, M. F. (2002), *Appl. Environ. Microbiol.* **68,** 1604–1609.
13. Verho, R., Londesborough, J., Penttilä, M., and Richard, P. (2003), *Appl. Environ. Microbiol.* **69,** 5892–5897.
14. Roca, C., Haack, M. B., and Olsson, L. (2004), *Appl. Microbiol. Biotechnol.* **63,** 578–583.
15. Kostrzynska, M., Sopher, C. R., and Lee, H. (1998), *FEMS Microbiol. Lett.* **159,** 107–112.
16. Metzger, M. H. and Hollenberg, C. P. (1995), *Eur. J. Biochem.* **228,** 50–54.
17. Watanabe, S., Kodaki, T., and Makino, K. (2005), *J. Biol. Chem.* **280,** 10,340–10,349.
18. Petschacher, B., Leitgeb, S., Kavanagh, K. L., Wilson, D. K., and Nidetzky, B. (2005), *Biochem. J.* **385,** 75–83.
19. Roca, C., Nielsen, J., and Olsson, L. (2003), *Appl. Environ. Microbiol.* **69,** 4732–4736.
20. Aristidou, A., Londesborough, J., Penttilä, M., Richard, P., Ruohonen, L., Söderlund, H., Teleman, A., and Toivari, M. H. (1999), Patent WO 99/46363 PCT/FI99/00185.
21. Kuyper, M., Harhangi, H. R., Stave, A. K., Winkler, A. A., Jetten, M. S. M., de Laat, W. T. A. M., den Ridder, J. J. J., Op den Camp, H. J. M., van Dijken, J. P., and Pronk, J. T. (2003), *FEMS Yeast Res.* **4,** 69–78.
22. Kuyper, M., Winkler, A. A., van Dijken, J. P., and Pronk, J. T. (2004), *FEMS Yeast Res.* **4,** 655–664.
23. Kuyper, M., Hartog, M. M. P., Toirkens, M. J., Almering, M. J. H., Winkler, A. A., van Dijken, J. P., and Pronk, J. T. (2005), *FEMS Yeast Res.* **5,** 399–409.
24. Pitkänen, J.-P., Aristidou, A., Salusjärvi, L., Ruohonen, L., and Penttilä, M. (2003), *Metab. Eng.* **5,** 16–31.
25. Salusjärvi, L., Poutanen, M., Pitkänen, J.-P., Koivistoinen, H., Aristidou, A., Kalkkinen, N., Ruohonen, L., and Penttilä, M. (2003), *Yeast* **20,** 295–314.
26. Palková, Z., Devaux, F., Ricicova, M., Minarikova, L., Le Crom, S., and Jacq, C. (2002), *Mol. Biol. Cell* **13,** 3901–3914.
27. Boles, E., Gohlmann, H. W., and Zimmermann, F. K. (1996), *Mol. Microbiol.* **20,** 65–76.
28. Ruohonen, L., Aalto, M. K., and Keränen, S. (1995), *J. Biotechnol.* **39,** 193–203.
29. Gietz, R. D. and Sugino, A. (1988), *Gene* **74,** 527–534.
30. Nadon, R. and Shoemaker, J. (2002), *Trends Genet.* **18,** 265–271.
31. Benjamini, Y. and Hochberg, Y. (1995), *J. R. Stat. Soc. Ser. B Method* **57,** 289–300.
32. Sambrook, J., Fritsch, E. F., and Maniatis, T. (1989), *A Laboratory Manual*, Cold Spring Harbor Laboratory, Cold Spring Harbor, NY.
33. Pitkänen, J.-P., Rintala, E., Aristidou, A., Ruohonen, L., and Penttilä, M. (2005), *Appl. Microbiol. Biotechnol.* **67,** 827–837.
34. Meijer, M. M., Boonstra, J., Verkleij, A. J., and Verrips, C. T. (1998), *J. Biol. Chem.* **273,** 24,102–24,107.
35. Herrero, P., Galindez, J., Ruiz, N., Martinez-Campa, C., and Moreno, F. (1995), *Yeast* **11,** 137–144.
36. Luttik, M. A., Kötter, P., Salomons, F. A., van der Klei, I. J., van Dijken, J. P., and Pronk, J. T. (2000), *J. Bacteriol.* **182,** 7007–7013.
37. Vuralhan, Z., Morais, M. A., Tai, S.-L., Piper, M. D. W., and Pronk, J. T. (2003), *Appl. Environ. Microbiol.* **69,** 4534–4541.
38. Delneri, D., Gardner, D. C., Bruschi, C. V., and Oliver, S. G. (1999), *Yeast (Chichester, West Sussex)* **15,** 1681–1689.
39. Dickinson, J. R., Salgado, L. E. J., and Hewlins, M. J. E. (2003), *J. Biol. Chem.* **278,** 8028–8034.
40. Daum, G., Lees, N. D., Bard, M., and Dickson, R. (1998), *Yeast (Chichester, West Sussex)* **14,** 1471–1510.
41. Swain, E., Stukey, J., McDonough, V., Germann, M., Liu, Y., Sturley, S. L., and Nickels, J. T. Jr. (2002), *J. Biol. Chem.* **277,** 36,152–36,160.

42. Balciunas, D., Galman, C., Ronne, H., and Björklund, S. (1999), *Proc. Natl. Acad. Sci. USA* **96,** 376–381.
43. Prelich, G. (1997), *Mol. Cell. Biol.* **17,** 2057–2065.
44. Geisberg, J. V., Holstege, F. C., Young, R. A., and Struhl, K. (2001), *Mol. Cell. Biol.* **21,** 2736–2742.
45. Lamb, T. M., Xu, W., Diamond, A., and Mitchell, A. P. (2001), *J. Biol. Chem.* **276,** 1850–1856.
46. Lyons, T. J., Gasch, A. P., Gaither, L. A., Botstein, D., Brown, P. O., and Eide, D. J. (2000), *Proc. Natl. Acad. Sci. USA* **97,** 7957–7962.
47. Tao, W., Deschenes, R. J., and Fassler, J. S. (1999), *J. Biol. Chem.* **274,** 360–367.
48. Brown, J. L., North, S., and Bussey, H. (1993), *J. Bacteriol.* **175,** 6908–6915.
49. Morgan, B. A., Bouquin, N., Merrill, G. F., and Johnston, L. H. (1995), *EMBO J.* **14,** 5679–5689.
50. Krems, B., Charizanis, C., and Entian, K.-D. (1996), *Curr. Genet.* **29,** 327–334.
51. Sato, T., Lopez, M. C., Sugioka, S., Jigami, Y., Baker, H. V., and Uemura, H. (1999), *FEBS Lett.* **463,** 307–311.
52. Akache, B., Wu, K., and Turcotte, B. (2001), *Nucleic Acids Res.* **29,** 2181–2190.
53. Sedlak, M., Edenberg, J. H., and Ho, N. W. Y. (2003), *Enzyme Microb. Technol.* **33,** 19–28.
54. Jin, Y.-S., Laplaza, J. M., and Jeffries, T. W. (2004), *Appl. Environ. Microbiol.* **70,** 6816–6825.
55. Wahlbom, C. F., Cordero Otero, R. R., van Zyl, W. H., Hahn-Hägerdal, B., and Jönsson, L. J. (2003), *Appl. Environ. Microbiol.* **69,** 740–746.
56. Sonderegger, M., Jeppsson, M., Hahn-Hägerdal, B., and Sauer, U. (2003), *Appl. Environ. Microbiol.* **70,** 2307–2317.
57. Daran-Lapujade, P., Jansen, M. L. A., Daran, J. M., van Gulik, W. M., de Winde, J. H., and Pronk, J. T. (2004), *J. Biol. Chem.* **5,** 9125–9138.
58. Elbing, K., Larsson, C., Bill, R. M., Albers, E., Snoep, J. L., Boles, E., Hohmann, S., and Gustafsson, L. (2004), *Appl. Environ. Microbiol.* **70,** 5323–5330.
59. Elbing, K., Stahlberg, A., Hohmann, S., and Gustafsson, L. (2004), *Eur. J. Biochem.* **271,** 4855–4864.
60. Bakker, B. M., Bro, C., Kötter, P., Luttik, M. A., van Dijken, J. P., and Pronk, J. T. (2000), *J. Bacteriol.* **182,** 4730–4737.
61. Satrustegui, J., Bautista, J., and Machado, A. (1983), *Mol. Cell Biochem.* **51,** 123–127.
62. Belinchón, M. M. and Gancedo, J. M. (2003), *Arch. Microbiol.* **180,** 293–297.
63. Young, E. T., Dombek, K. M., Tachibana, C., and Ideker, T. (2003), *J. Biol. Chem.* **278,** 26,146–26,158.
64. Dahlquist, K. D., Salomonis, N., Vranizan, K., Lawlor, S. C., and Conklin, B. R. (2002), *Nat. Genet.* **31,** 19, 20.
65. Cheng, C., Kacherovsky, N., Dombek, K. M., Camier, S., Thukral, S. K., Rhim, E., and Young, E. T. (1994), *Mol. Cell. Biol.* **14,** 3842–3852.
66. Schöler, A. and Schüller, H. J. (1994), *Mol. Cell. Biol.* **14,** 3613–3622.
67. Bram, R. J., Lue, N. F., and Kornberg, R. D. (1986), *EMBO J.* **5,** 603–608.
68. Lundin, M., Nehlin, J. O., and Ronne, H. (1994), *Mol. Cell. Biol.* **14,** 1979–1985.
69. Martinez-Pastor, M. T., Marchler, G., Schüller, C., Marchler-Bauer, A., Ruis, H., and Estruch, F. (1996), *EMBO J.* **15,** 2227–2235.
70. Ogawa, N., Saitoh, H., Miura, K., Magbanua, J. P., Bun-ya, M., Harashima, S., and Oshima, Y. (1995), *Mol. Gen. Genet.* **249,** 406–416.

Supplemental Table 1
Genes With Increased Expression on Xylose

ORF ID	Gene	Fold change	Description
			Amino acid metabolism
YJL088w	*ARG3*	1.9	Ornithine carbamoyltransferase
YHR137w	*ARO9*	6.7	Aromatic amino acid aminotransferase II
YLL062c	*MHT1*	5.0	*S*-methylmethionine homocysteine methyl transferase
YBR006w	*UGA2*	4.4	Succinate semialdehyde dehydrogenase
YFR055w		3.8	Strong similarity to β-cystathionases
			Cell cycle and differentiation
YGR140w	*CBF2*	7.0	Kinetochore protein complex CBF3, 110-kDa subunit
YPR025c	*CCL1*	23.7	TFIIH subunit (transcription initiation factor), cyclin C component
YFL009w	*CDC4*	3.8	Cell division control protein
YGL190c	*CDC55*	16.6	ser/thr phosphatase 2A regulatory subunit B, involved in cellular morphogenesis
YLR433c	*CNA1*	9.3	Calcineurin B, catalytic subunit
YBR040w	*FIG1*	2.7	Required for efficient mating
YNL307c	*MCK1*	22.3	ser/thr/tyr protein kinase
YEL032w	*MCM3*	2.0	Replication initiation protein
YER044c-a	*MEI4*	52.6	Meiosis-specific protein
YEL019c	*MMS21*	10.2	DNA repair protein
YGR049w	*SCM4*	6.5	CDC4 suppressor
YHR206w	*SKN7*	2.4	Transcription factor with similarity to Hsf1p
YPR054w	*SMK1*	14.1	Sporulation-specific mitogen-activated protein kinase
			Classification not yet clear
YDL214c	*PRR2*	2.9	Strong similarity to putative protein kinase Npr1
YER089c	*PTC2*	20.3	Protein serine/threonine phosphatase of PP2C family
			C-compound and carbohydrate utilization
YNL331c	*AAD14*	27.9	Strong similarity aryl-alcohol reductase
YAL054c	*ACS1*	4.0	Acetyl-CoA synthetase
YOR374w	*ALD4*	5.1	Aldehyde dehydrogenase, mitochondrial

YPL061w	*ALD6*	6.3	Aldehyde dehydrogenase, cytosolic
YDR380w	*ARO10*	4.4	Similarity to Pdc6p, Thi3p, and pyruvate decarboxylases
YML054c	*CYB2*	2.1	Lactate dehydrogenase cytochrome b2
YBR020w	*GAL1*	2.5	Galactokinase
YHR183w	*GND1*	1.9	6-Phosphogluconate dehydrogenase
YPR006c	*ICL2*	4.9	2-Methylisocitrate lyase
			Control of cellular organization
YKL096w-a	*CWP2*	1.9	Cell wall mannoprotein
YNR030w	*ECM39*	3.2	Involved in cell wall biogenesis and architecture
YLR425w	*TUS1*	3.4	TOR Unique function Suppressor; exchange factor for Rho1p, cell wall integrity
			Detoxification
YDR256c	*CTA1*	4.3	Catalase A, peroxisomal
YMR038c	*LYS7*	3.5	Copper chaperone for superoxide dismutase Sod1p
YER185w		3.6	Strong similarity to Rtm1p, a protein that confers resistance to molasses
			Homeostasis of ions
YLR433c	*CNA1*	9.3	Calcineurin B, catalytic subunit
YPR124w	*CTR1*	10.5	Copper transport protein
YEL027w	*CUP5*	13.4	H^+-ATPase V0 domain 17-kDa subunit, vacuolar
YMR038c	*LYS7*	3.5	Copper chaperone for superoxide dismutase Sod1p
YML123c	*PHO84*	3.2	High-affinity inorganic phosphate/H^+ symporter
YBR106w	*PHO88*	2.7	Involved in phosphate transport
YBR296c	*PHO89*	3.7	Na^+-coupled phosphate transport protein, high affinity
YLR447c	*VMA6*	3.7	H^+-ATPase V0 domain 36-kDa subunit, vacuolar
YGL255w	*ZRT1*	15.6	High-affinity zinc transport protein
YLR130c	*ZRT2*	2.8	Low-**affinity** zinc transporter
YKL175w	*ZRT3*	2.2	Vacuolar membrane protein involved in regulation of zinc storage
			Lipid fat and isoprenoid metabolism
YGR175c	*ERG1*	2.8	Squalene monooxygenase
YHR007c	*ERG11*	3.1	Cytochrome P450 lanosterol 14a-demethylase
YGR060w	*ERG25*	3.3	C-4 sterol methyl oxidase

(continued)

Supplemental Table 1 *(continued)*

ORF ID	Gene	Fold change	Description
YMR015c	*ERG5*	2.7	C-22 sterol desaturase
YML008c	ERG6	2.4	*S*-adenosyl-methionine δ-24-sterol-c-methyltransferase
YKR009c	*FOX2*	2.1	Hydratase-dehydrogenase-epimerase, peroxisomal
YLR099c	*ICT1*	3.3	Similarity to YDR125c, a protein involved in cell wall organization
YNR008w	*LRO1*	6.6	A lecithin cholesterol acyltransferase-like gene, mediates diacylglycerol esterification
YMR006c	*PLB2*	2.6	Strong similarity to phospholipase B (Plb1p and YOL011w)
			Metabolism of vitamins, cofactors, and prosthetic groups
YOL151w	*GRE2*	3.9	Similarity to plant dihydroflavonol-4-reductases
			Nucleotide metabolism
YER060w	*FCY21*	12.2	Purine-cytosine permease
YMR287c	*MSU1*	3.3	3'-5' Exonuclease for RNA 3' ss-tail, mitochondrial
YDL244w	*THI13*	3.9	Strong similarity to THI5P, YJR156c, and YNL332w involved in thiamine biosynthesis
			Protein synthesis
YHR011w	*DIA4*	2.7	Strong similarity to seryl-tRNA synthetases
YER117w	*RPL23B*	4.9	Ribosomal protein L23.e
YGR148c	*RPL24B*	2.2	60S large subunit ribosomal protein L24.e.B
YDL136w	*RPL35B*	2.3	60S large subunit ribosomal protein
YGL147c	*RPL9A*	3.2	Ribosomal protein L9.e
YOL121c	*RPS19A*	4.3	40S small subunit ribosomal protein S19.e
YJL190c	*RPS22A*	4.4	Ribosomal protein S15a.e.c10
YBL072c	*RPS8A*	2.0	Ribosomal protein S8.e
			Regulation of C-compound and carbohydrate metabolism
YOR344c	*TYE7*	3.1	Basic helix-loop-helix transcription factor, needed for maximal expression of enolase
YFL052w		5.4	Strong similarity to Mal63p, YPR196w, and Mal13p
			Respiration
YML054c	*CYB2*	2.1	Lactate dehydrogenase cytochrome b2
YKL055c	*OAR1*	3.2	Putative 3-oxoacyl-(acyl carrier protein) reductase

			Stress response and protein folding
YGL190c	*CDC55*	16.6	ser/thr phosphatase 2A regulatory subunit B
YBR201w	*DER1*	2.9	Involved in degradation proteins in the endoplasmic reticulum
YBL040c	*ERD2*	5.2	Endoplasmic reticulum lumen protein-retaining receptor
YMR038c	*LYS7*	3.5	Copper chaperone for superoxide dismutase Sod1p
YPL085w	*SEC16*	4.2	Multidomain vesicle coat protein
YHR206w	*SKN7*	2.4	Transcription factor with similarity to heat-shock transcription factor Hsf1p
YBR067c	*TIP1*	3.0	Cell wall mannoprotein with lipase activity
YLR417w	*VPS36*	24.9	Defective in vacuolar protein sorting
			Transcription
YPR057w	*BRR1*	14.1	Involved in snRNP biogenesis
YER159c	*BUR6*	2.4	Functional homolog of human NC2α, transcriptional regulator
YPR025c	*CCL1*	23.7	TFIIH subunit (transcription initiation factor), cyclin C component
YLR433c	*CNA1*	9.3	Calcineurin B, catalytic subunit, may be involved in regulation of some ion pumps
YBR020w	*GAL1*	2.5	Galactokinase
YPR068c	*HOS1*	11.7	Histone deacetylase
YPR070w	*MED1*	22.3	Component of RNA polymerase II holoenzyme and mediator subcomplex
YBR193c	*MED8*	2.8	RNA polymerase II transcriptional regulation mediator
YMR287c	*MSU1*	3.3	3'-5' Exonuclease for RNA 3' ss-tail, mitochondrial
YBR066c	*NRG2*	3.4	Weak similarity to *Aspergillus niger* carbon catabolite repressor protein, interacts with Snf1p
YHR206w	*SKN7*	2.4	Transcription factor with similarity to Hsf1p (osmotic and oxidative stress)
YPR086w	*SUA7*	6.2	TFIIB subunit (transcription initiation factor), factor E
YKL058w	*TOA2*	2.0	TFIIA subunit (transcription initiation factor), 13.5 kDa
YOR344c	*TYE7*	3.1	Basic helix-loop-helix transcription factor
YJL056c	*ZAP1*	3.0	Metalloregulatory protein involved in zinc-responsive transcriptional regulation
YFL052w		5.4	Strong similarity to Mal63p, YPR196w, and Mal13p
YER130c		2.4	Similarity to Msn2p and weak similarity to Msn4p
			Transport facilitation
YLR242c	*ARV1*	5.5	Involved in sterol uptake and distribution into plasma membrane
YCR010c	*ATO1*	11.7	Member of YaaH family of putative transporters

(continued)

Supplemental Table 1 *(continued)*

ORF ID	Gene	Fold change	Description
YNR002c	*ATO2*	15.8	Member of YaaH family of putative transporters
YDR384c	*ATO3*	3.8	Member of YaaH family of putative transporters
YER060w	*FCY21*	12.2	Purine-cytosine permease
YKR039w	*GAP1*	3.7	General amino acid permease
YPL189w	*GUP2*	13.7	Putative glycerol transporter involved in active glycerol uptake
YMR011w	*HXT2*	5.2	High-affinity hexose transporter
YKL217w	*JEN1*	3.0	Carboxylic acid transporter protein
YKL057c	*NUP120*	3.2	Nuclear pore protein
YPL058c	*PDR12*	8.4	Multidrug resistance transporter
YFL054c		4.1	Similarity to channel proteins
			Transposons
YCL020W		4.4	TyA Gag protein
YJL113W		5.6	TyB Gag-Pol protein
YML040W		2.7	TyA Gag protein
YML045W		2.4	TyB Gag-Pol protein
			Unclassified
YKL219w	*COS9*	7.1	Similarity to subtelomeric encoded proteins
YML006c	*GIS4*	50.3	Suppressor of Gig3 cyclin-dependent protein kinase
YBR066c	*NRG2*	3.4	Weak similarity to *Aspergillus niger* carbon catabolite repressor protein, interacts with Snf1
YAL046c		2.7	Unknown function
YBR005w		2.5	Strong similarity to hypothetical protein YDR003w
YCR090c		6.2	Similarity to *Schizosaccharomyces pombe* SPBC2D10.03c
YDR412w		18.3	Unknown function
YDR525w		5.5	Hypothetical protein
YEL041w		5.6	Strong similarity to Utr1p involved in iron homeostasis
YER076c		3.3	Similarity to killer toxin Khr1p
YER152c		3.2	Weak similarity to *Escherichia coli* hypothetical protein f470
YGR161c		2.6	Hypothetical protein

YIL057c		11.6	Strong similarity to unknown protein YER067w
YJR013w		4.5	Similarity to *Caenorhabditis elegans* B0491.1 protein
YLR302c		2.5	Unknown function
YML010W-A		9.4	Protein of unknown function
YML041c		11.5	Weak similarity to probable cyclin G1 interacting protein *Schizosaccharomyces pombe*
YMR082c		10.6	Hypothetical protein
YMR107w		12.7	Hypothetical protein
YMR316c-a		36.1	Unknown function
YNL028w		30.2	Unknown function
YOL101c		3.6	Similarity to YOL002c involved in PHO signaling pathway
YOL107w		3.6	Weak similarity to human PL6 protein
YOL154w	*ZPS1*	59.1	Putative GPI-anchored protein, transcription induced under low zinc and alkaline pH
YPL073c		110.8	Unknown function
YPL137c		16.2	Similarity to microtubule-interacting protein Mhp1p and to hypothetical protein YOR227w
YPR038w		132.1	Unknown function
YPR118w		2.5	Similarity to *Methanocaldococcus jannaschii* translation initiation factor, eIF-2B
			Vesicular transport
YBL040c	*ERD2*	5.2	Endoplasmic reticulum lumen protein-retaining receptor
YPL085w	*SEC16*	4.2	Multidomain vesicle coat protein

Supplemental Table 2
Genes with Decreased Expression on Xylose

ORF ID	Gene	Fold change	Description
			Amino acid metabolism
YHR018c	*ARG4*	3.6	Arginosuccinate lyase
YDR019c	*GCV1*	3.0	Glycine decarboxylase, subunit T
YCL018w	*LEU2*	2.6	β-Isopropyl-malate dehydrogenase
			Cell cycle and differentiation
YNR044w	*AGA1*	2.5	a-Agglutinin anchor subunit
YBL085w	*BOI1*	2.9	Bem1 protein-binding protein
YGR023w	*MTL1*	2.7	Potential cell wall stress sensor
YJL079c	*PRY1*	2.2	Strong similarity to the plant PR-1 class of pathogen-related proteins
YDR388w	*RVS167*	3.7	Reduced viability on starvation protein
YJR004c	*SAG1*	3.3	α-Agglutinin
YKL178c	*STE3*	2.3	Pheromone a-factor receptor
YJR066w	*TOR1*	2.8	Phosphatidylinositol 3-kinase
			Classification not yet clear
YOR383c	*FIT3*	3.7	Weak similarity to *Leishmania mexicana* secreted acid phosphatase 2
YCR091w	*KIN82*	3.7	ser/thr protein kinase
			C-compound and carbohydrate utilization
YBL015w	*ACH1*	2.2	Acetyl-CoA hydrolase
YMR170c	*ALD2*	5.3	Aldehyde dehydrogenase 2 (NAD^+)
YMR169c	*ALD3*	13.1	Stress-inducible aldehyde dehydrogenase
YAL060w	*BDH1*	2.3	Stereospecific (2*R*, 3*R*)-2,3-butanediol dehydrogenase
YPL262w	*FUM1*	2.6	Fumarate hydratase
YEL011w	*GLC3*	4.0	1,4-Glucan-branching enzyme (glycogen-branching enzyme)
YHR104w	*GRE3*	2.9	Aldose reductase
YGR032w	*GSC2*	2.2	1,3-β-D-glucan synthase subunit
YFR053c	*HXK1*	2.4	Hexokinase I
YER065c	*ICL1*	3.7	Isocitrate lyase
YOR136w	*IDH2*	2.0	Isocitrate dehydrogenase (NAD^+) subunit 2, mitochondrial

YIL125w	*KGD1*	2.5	2-Oxoglutarate dehydrogenase complex E1 component
YDR148c	*KGD2*	2.3	2-Oxoglutarate dehydrogenase complex E2 component
YGR292w	*MAL12*	2.2	α-D-Glucosidase of MAL1 locus
YBR299w	*MAL32*	4.0	α-D-Glucosidase
YKL085w	*MDH1*	2.6	Malate dehydrogenase precursor, mitochondrial
YMR105c	*PGM2*	12.0	Phosphoglucomutase, major isoform
YIL045w	*PIG2*	7.6	Protein interacting with glycogen synthase Gsy2p
YBR126c	*TPS1*	3.3	α,α-Trehalose-phosphate synthase, 56-kDa subunit
YDR074w	*TPS2*	2.1	α,α-Trehalose-phosphate synthase, 102-kDa subunit
YML100w	*TSL1*	11.0	α,α-Trehalose-phosphate synthase, 123-kDa subunit
YKL035w	UGP1	4.0	UTPglucose-1-phosphate uridylyltransferase
YGR287c		4.3	Strong similarity to maltase
YAL061w		4.8	Putative polyol dehydrogenase
			Control of cellular organization
YER150w	*SPI1*	5.1	Stationary Phase Induced protein
			Detoxification
YHR053c	*CUP1-1*	6.3	Metallothionein
YHR055c	*CUP1-2*	11.8	Metallothionein
YOL158c	*ENB1*	2.9	A transporter for enterobactin encoded by a gene of major facilitator superfamily
YIL120w	*QDR1*	5.2	Similarity to antibiotic resistance proteins
YEL065w	*SIT1*	2.8	Probable multidrug resistance protein
YJR104c	*SOD1*	3.1	Copper-zinc superoxide dismutase
YHR008c	*SOD2*	2.9	Superoxide dismutase (Mn) precursor, mitochondrial
YGR138c	*TPO2*	3.2	Polyamine transport protein
			Homeostasis of ions
YLR109w	*AHP1*	2.3	Alkyl hydroperoxide reductase
YMR058w	*FET3*	3.0	Cell-surface ferroxidase, high affinity
YFL041w	*FET5*	3.1	Multicopy oxidase
YBR207w	*FTH1*	5.5	Similarity to iron permease Ftr1p (YER145c)
YER145c	*FTR1*	2.1	Iron permease that mediates high-affinity iron uptake
YDR456w	*NHX1*	3.6	NA^+-H^+ antiporter
YEL065w	*SIT1*	2.8	Probable multidrug resistance protein
YGL096w	*TOS8*	3.3	Similarity to copper homeostasis protein Cup9p

(continued)

Supplemental Table 2 *(continued)*

ORF ID	Gene	Fold change	Description
			Oxidation of fatty acids
YNL202w	*SPS19*	44.2	Peroxisomal 2,4-dienoyl-CoA reductase
			Stress response and protein folding
YLR109w	*AHP1*	2.3	Alkyl hydroperoxide reductase
YDR358w	*GGA1*	2.4	Arf-binding protein involved in trafficking of proteins
YHR104w	*GRE3*	2.9	Aldose reductase
YLL026w	*HSP104*	10.6	Heat-shock protein
YDR171w	*HSP42*	3.0	Weak similarity to *Streptomyces* Hsp18 protein
YDR258c	*HSP78*	2.9	Heat-shock protein of clpb family of adenosine triphosphate–dependent proteases, mitochondrial
YPL240c	*HSP82*	3.1	Heat-shock protein
YFL016c	*MDJ1*	5.3	Heat-shock protein-chaperone
YDR033w	*MRH1*	2.6	Membrane protein related to Hsp30p
YDR494w	*RSM28*	3.6	Mitochondrial small subunit protein
YBR214w	*SDS24*	4.0	Strong similarity to hypothetical protein YGL056c
YLL024c	*SSA2*	2.0	Heat-shock protein of Hsp70 family, cytosolic
YER098w	*UBP9*	3.6	Ubiquitin carboxyl-terminal hydrolase
YKL035w	*UGP1*	4.0	UTPglucose-1-phosphate uridylyltransferase
YNL160w	*YGP1*	5.6	Secreted glycoprotein
YGR234w	*YHB1*	3.0	Flavohemoglobin
YBR054w	*YRO2*	3.0	Strong similarity to Hsp30 heat-shock protein Yro1p
			Transcription
YKL043w	*PHD1*	2.0	Transcription factor
YHR056c	*RSC30*	6.3	RSC complex component
YKR092c	*SRP40*	2.1	Suppressor of mutant AC40 of RNA polymerase I and III
YDL048c	*STP4*	4.8	Involved in pre-tRNA splicing and in uptake of branched-chain amino acids
YLR136c	*TIS11*	3.0	tRNA-specific adenosine deaminase 3
			Transport facilitation
YHL040c	*ARN1*	3.1	Ferrichrome-type siderophore transporter
YOL158c	*ENB1*	2.9	A transporter for enterobactin encoded by a gene of major facilitator superfamily
YMR058w	*FET3*	3.0	Cell-surface ferroxidase, high affinity

YFL041w	*FET5*	3.1	Multicopy oxidase
YBR207w	*FTH1*	5.5	Similarity to iron permease Ftr1p (YER145c)
YER145c	*FTR1*	2.1	Iron permease that mediates high-affinity iron uptake
YBR298c	*MAL31*	6.0	Maltose permease
YDR456w	*NHX1*	3.6	NA^{+}-H^{+} antiporter
YKL198c	*PTK1*	24.2	Polyamine transport-enhancing protein
YKR093w	*PTR2*	2.6	Peptide transporter
YIL120w	*QDR1*	5.2	Similarity to antibiotic resistance proteins
YEL065w	*SIT1*	2.8	Probable multidrug resistance protein
YGR138c	*TPO2*	3.2	Polyamine transport protein
YHL035c		3.3	Similarity to multidrug resistance proteins
			Unclassified
YDR511w	*ACN9*	4.9	Weak similarity to *Caenorhabditis elegans* protein F25H9.7
YDR534c	*FIT1*	10.4	Similarity to Fit3p involved in iron transport
YOR382w	*FIT2*	2.8	Hypothetical protein
YML128c	*MSC1*	4.7	Weak similarity to *Schizosaccharomyces pombe* SPBC365.12c protein of unknown function
YLR265c	*NEJ1*	6.5	Hypothetical protein
YOL084w	*PHM7*	3.6	Similarity to *Arabidopsis thaliana* hyp1 protein
YEL035c	*UTR5*	2.8	Weak similarity to *Neisseria gonorrhoeae* PilG protein
YBR116c		11.5	Questionable ORF
YCL042w		2.6	Questionable ORF
YDL204w		9.0	Similarity to hypothetical protein YDR233c
YDL222c		18.3	Strong similarity to hypothetical protein YNL194c
YER067w		18.0	Strong similarity to hypothetical protein YIL057c
YFR039c		2.6	Similarity to hypothetical protein YGL228w
YGR031w		2.8	Weak similarity *Haemophilus influenzae* dihydrolipoamide acetyltransferase
YGR235c		3.2	Hypothetical protein
YHL021c		3.4	Weak similarity to *Pseudomonas* γ-butyrobetaine hydroxylase
YHR087w		5.3	Weak similarity to PIR:T50363 hypothetical protein SPBC21C3.19 *Schizosaccharomyces pombe*
YKL044w		2.5	Hypothetical protein
YLR205c		2.0	Hypothetical protein
YLR456w		24.4	Strong similarity to hypothetical ORF YPR172w
YLR464w		2.8	Strong similarity to subtelomeric encoded proteins
YMR172c-a		41.0	Questionable ORF

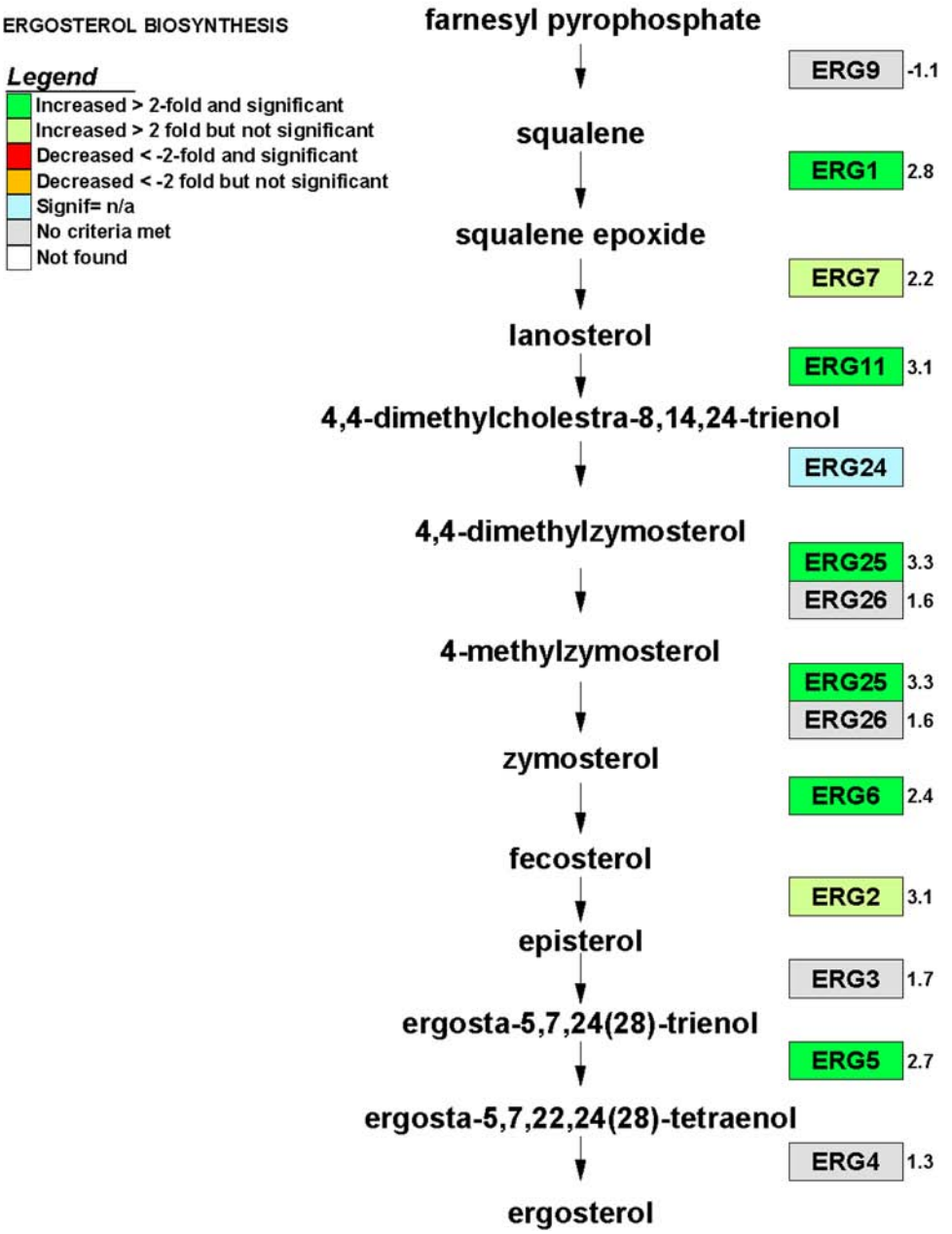

Supplemental Fig. 1. Schematic representation of ergosterol biosynthesis in yeast. Expression ratios are marked next to the genes; positive values indicate upregulation and negative values downregulation on xylose. Dark green shows statistically significantly increased expression levels in xylose culture compared to glucose, and light green more than twofold increased expression that, however, was not statistically significant. Expression levels of genes marked in gray did not change. Blue indicates that no signal was detected and white that the ORF was absent from the array. The figures were drawn using GenMAPP software (www.genmapp.org) *(64)*.

Supplemental Table 3
Promoter Elements of Transcription Factors in Promoter Areas (–800 bp) of 125 Genes Upregulated on Xylose (A) and 100 Genes Downregulated on Xylose (B), and of All 6144 Genes on an Array (C)[a]

Transcription factor	Description	Promoter element[b]	A (gene coverage [%])	B (gene coverage [%])	C (array coverage [%])	Reference
Adr1p	Promotes expression of *ADH2*, of genes encoding peroxisomal proteins, and of genes encoding activities required for ethanol, glycerol, and fatty acid utilization	TTGGrG	18	9	13	*66*
Cat8p[c]	Involved in activation of expression of genes encoding key gluconeogenic enzymes	yCCrTTnrnCCG	1	1	2	*67*
Gal4p	Positive regulator of expression of *GAL* genes	CGG(n)^{11}CCG	7	6	5	*68*
Mig1p[c]	Major transcription factor mediating glucose repression	(w)^{5}nsyGGGG	11	9	4	*69*
Msn2p/Msn4p	Key regulator and activator of stress-responsive gene expression	AGGGG	14	45	16	*70*
Pho4p	Transcription factor that activates expression of phosphate pathway	GCACGT(k)^{3}	2	0	0.2	*71*
Zap1p[c,d]	Metalloregulatory protein involved in zinc-responsive transcriptional activation	ACCTTnAAGGT	6	3	3	*47*

[a]Except for Cat8p, Mig1p, and Zap1p, only the genes with promoter regions containing at least two copies of the regulatory element are included. Among the genes encoding the transcription factors presented in the table, only *ZAP1* had an altered expression level of statistical significance between the xylose and glucose culture (threefold upregulation on xylose; *see* Table 1).

[b]Redundant nucleotides: n = any nucleotide; k = G or T; m = A or C; r = A or G; s = G or C; w = A or T; y = C or T.

[c]Genes with only one promoter element also included.

[d]One base substitution allowed within promoter element.